

# Convective Weather Avoidance Prediction in Enroute Airspace Based on Support Vector Machine

LI Jiahao<sup>1</sup>, WANG Shijin<sup>1\*</sup>, CHU Jiewen<sup>1</sup>, LIN Jingjing<sup>2</sup>, WEI Chunjie<sup>3</sup>

1. College of Civil Aviation, Nanjing University of Aeronautics and Astronautics, Nanjing 211106, P. R. China;

2. Nanjing Les Information Technology Co., Ltd, Nanjing 210014, P. R. China;

3. Jiangsu Sub-bureau of East China Regional Air Traffic Management Bureau, Nanjing 211113, P. R. China

(Received 2 June 2021; revised 20 July 2021; accepted 31 July 2021)

**Abstract:** With the rapid growth of global air traffic, flight delays are increasingly serious. Convective weather is one of the influential causes for flight delays, which has affected the sustainable development of civil aviation industry and became a social problem. If it can be predicted that whether a weather-related flight diverts, participants in air traffic activities can coordinate the scheduling, and flight delays can be reduced greatly. In this paper, the weather avoidance prediction model (WAPM) is proposed to find the relationship between weather and flight trajectories, and predict whether a future flight diverts based on historical flight data. First, given the large amount of weather data, the principal component analysis is used to reduce the ten dimensional weather indicators to extract 90% information. Second, the support vector machine is adopted to predict whether the flight diverts by determining the hyperparameters  $c$  and  $\gamma$  of the radial basis function. Finally, the performance of the proposed model is evaluated by prediction accuracy, precision, recall and  $F_1$ , and compared with the methods of the  $k$  nearest neighbor (kNN), the logistic regression (LR), the random forest (RF) and the deep neural networks (DNNs). WAPM's accuracy is 5.22%, 2.63%, 2.26% and 1.03% greater than those of kNN, LR, RF and DNNs, respectively; WAPM's precision is 6.79%, 5.19%, 4.37% and 3.21% greater than those of kNN, LR, RF and DNNs, respectively; WAPM's recall is 4.05%, 1.05%, 0.04% greater than those of kNN, LR, and RF, respectively, and 1.38% lower than that of the DNNs; and  $F_1$  of WAPM is 5.28%, 1.69%, 1.98% and 0.68% greater than those of kNN, LR, RF and DNNs, respectively.

**Key words:** convective weather; avoidance prediction; data mining; evaluation indicator; enroute airspace

**CLC number:** V355

**Document code:** A

**Article ID:** 1005-1120(2021)04-0656-15

## 0 Introduction

With the rapid growth of global air traffic, the problem of flight delay is increasingly serious. According to data released by the Civil Aviation Administration of China, flight delays caused by weather accounts for 56.52%, 51.28%, 47.46%, 46.49%, 57.31% of the total number of each year from 2016 to 2020<sup>[1]</sup>. In the US National Airspace System (NAS), weather is responsible for over 70% of the delays and convective weather for 60%

of them<sup>[2]</sup>. Convective weather is one of the influential factors for flight delays and cancellations. The large amount of flight delays leads to pressure and economic loss for airlines, air traffic management units, airports, etc, and affects the sustainable development of the civil aviation industry. It has become a social problem. If the strategic, pre-tactical and tactical weather forecast can help to predict whether a weather-related flight diverts, participants in air traffic activities can coordinate the sched-

\*Corresponding author, E-mail address: shijin\_wang@nuaa.edu.cn.

**How to cite this article:** LI Jiahao, WANG Shijin, CHU Jiewen, et al. Convective weather avoidance prediction in enroute airspace based on support vector machine[J]. Transactions of Nanjing University of Aeronautics and Astronautics, 2021, 38(4):656-670.

<http://dx.doi.org/10.16356/j.1005-1120.2021.04.012>

uling. And the predicted results will provide decision support to air traffic management departments and airlines by planning diversion paths, thus to greatly reduce flight delays and workloads of controllers.

At present, the research of weather avoidance is devoted to air traffic management, including weather avoidance prediction, weather avoidance probability and airspace availability.

In weather avoidance prediction research, most studies used weather features and flight features. DeLaura et al. in 2006<sup>[3]</sup> and 2008<sup>[4]</sup> proposed an approach that avoids convective weather using different weather features by the Gaussian discriminant analysis (GDA) and the  $k$  nearest neighbor (kNN) methods, and the prediction error was approximately 25%. In 2013, Stewart et al.<sup>[5]</sup> predicted weather avoidance by evaluating flight types, operation types, flight stages, take-off and landing facilities, and weather avoidance behaviors. Their probability of weather avoidance was approximately 59%. The research of weather avoidance probability is to establish weather avoidance field (WAF) by weather avoidance prediction to reflect the probability of aircraft diversion under different weather conditions. Most studies used the convective weather avoidance model (CWAM) to establish WAF. In 2010, Matthews et al.<sup>[6]</sup> used probability of correct deviation prediction (PoD), false alarm rate (FAR) and critical skill index (CSI) to evaluate four different CWAMs. The performance difference between the models was almost insignificant, and the probability of correct deviation prediction was 65%. In 2012, Campbell et al.<sup>[7]</sup> used detection probability and FAR to evaluate the effectiveness of CWAM in arrival traffic. Airspace availability can be used to judge the influence degree of convective weather on the airspace and predict whether the flight is diverted. It is represented by blocking or permeability, that is, the probability of traffic flow being blocked and permeated per unit time. In 2016, Matthews et al.<sup>[8]</sup> adopted the supervised machine learning method based on the multiple meteorological sources data

to develop the airspace permeability calculation model under convective weather and to forecast the permeability in the next 12 hours. In 2014, Ye et al.<sup>[9]</sup> used the scanning method to segment the airspace based on the scanning baseline, set the blocking according to the video integrator processor (VIP) level, and then calculated the blocking in the airspace under convective weather in a specific direction.

Some studies<sup>[10-11]</sup> plan diversion routes and strategies for flights that avoid airspace affected by convective weather, and some other predictions under convective weather have been studied, including airport capacity<sup>[12]</sup>, delay<sup>[13]</sup>, and flight time prediction<sup>[14]</sup>. Most studies in China<sup>[15-16]</sup> have focused on diversion path planning and algorithms under convective weather, but seldom has looked into convective weather avoidance prediction.

Some limitations exist in the current weather avoidance prediction research: (1) The prediction model in foreign research may not be suitable for China, because the air traffic control operational regulations and the flying habits of pilots in China are different from those in other countries; (2) in terms of China's research, most of the research in this area focuses on diversion path planning and algorithms; and (3) the suitability of GDA for weather avoidance prediction in China is uncertain, so it is necessary to verify GDA suitability under China airspace situations.

Data mining is a process of searching hidden information and extracting it to obtain its internal relationships. In this paper, weather data, radar trajectory data and flight plan data are required for convective weather avoidance. The amount of required data is large, and there are various data categories that have abundant avoidance information. The effective historical experiences of controllers and pilot behaviors can be obtained through mining historical flight data. The weather data are processed for dimensionality reduction by the principal component analysis (PCA), and then are combined with radar trajectory data and flight plan data to establish the weather avoidance prediction model (WAPM) by the sup-

port vector machine (SVM), which can reflect the relationship between weather and flight trajectory. When future flights encounter convective weather, the decision of whether to avoid weather will be

made according to the intensity of the weather. The process of WAPM includes three stages: Historical data preparation, avoidance predictor, and simulation, as shown in Fig.1.

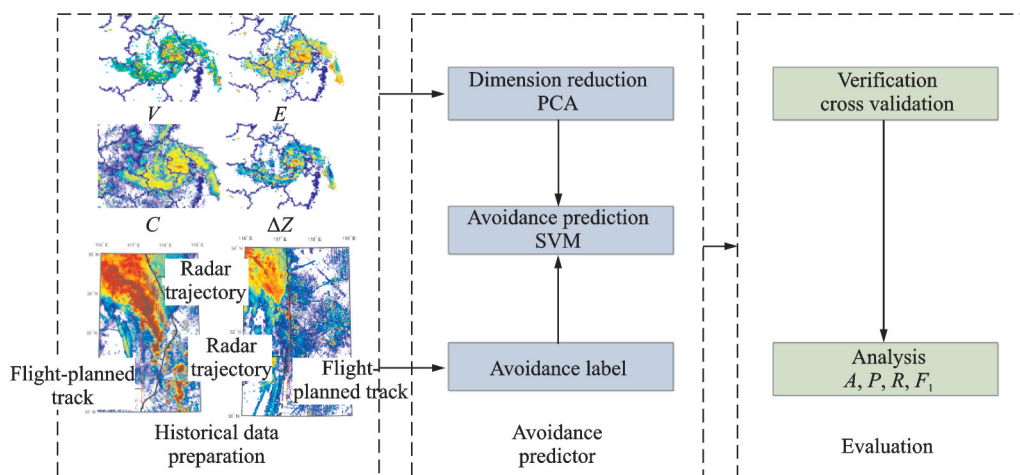


Fig.1 WAPM flow chart

## 1 Data Preparation

Each flight is carried out according to its flight plan that is made and published before departure. There are many factors that causes a flight not proceed as planned, including bad weather, flow control, and military activities. The actual flight trajectory is recorded in radar trajectory data. Weather data are used to reflect the weather severity in certain airspace. So convective weather avoidance judgment uses weather data, radar trajectory data and flight plan data.

### 1.1 Weather data

Convective weather occurs in mesoscale weather systems, which has strong destructiveness and threatens flight safety. Weather data can reflect the severity of convective weather and is provided by various weather products<sup>[17]</sup>.

Weather products are rooted from the reflectivity factor ( $Z$ ) obtained by Doppler radar. The value of three weather products combined reflectivity ( $C$ ), echo top ( $E$ ) and vertically integrated liquid ( $V$ ) are computed by reflectivity factor  $Z$ , and they are used to reflect the intensity, vertical structure and precipitation of convective weather, respectively. The resolution ratio of these weather data is

$0.01^\circ \times 0.01^\circ$  (longitude  $\times$  latitude). Weather product  $C$  reflects the intensity information of convective weather, and the unit of  $C$  is dBZ. A higher  $C$  value indicates greater convective weather intensity, as shown in Fig.2. Different colors can reflect the intensity of convective weather.  $E$  is the height of echo top, which indicates the height of convective weather, and the unit of  $E$  is m.  $V$  is the vertical accumulation of liquid water content, which indicates the precipitation of convective weather, and the unit of  $V$  is  $\text{kg}/\text{m}^2$ . A higher  $V$  value indicates bigger convective weather precipitation and higher probability of diversion. Therefore,  $C$ ,  $E$ , and  $V$  are selected for convective weather avoidance prediction.

$\Delta Z$  indicates the relationship between the flight level ( $L$ ) and the 90%  $E$ <sup>[3]</sup>, as described in Eq.(1).

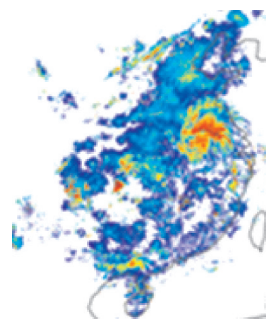


Fig.2 Weather chart of CR

The unit of  $\Delta Z$  is m. When  $\Delta Z$  is positive, it means that the flight is above the convective weather, whereas when  $\Delta Z$  is negative, the flight is more affected by convective weather.

$$\Delta Z = L - 90\%E \quad (1)$$

To fully reflect the intensity and range of the convective weather within a certain range of the airspace, the weather values in different percentiles can make the distribution more robust and can better represent the weather feature in a certain spatial filter. Therefore, ten weather indicators including the maximum, 90%, 50% of  $C$ ,  $E$ ,  $V$  and  $\Delta Z$  in certain airspace are selected and shown in Table 1. In statistics, the  $n$ th percentile of a set of data is the value at which  $n$  percent of the data is below it. The enroute is 10 km wide on both sides of the centerline. The spatial filter is an assigned airspace scope. The width of the spatial filter is the same as that of the enroute, and the length of it is the length between two adjacent waypoints of flight plan track, as shown in Fig.3. The corresponding percentiles are selected for the ten weather indicators, that is, the maximum, 90%, 50% of  $C$ ,  $E$ ,  $V$  and  $\Delta Z$  under spatial filter, and ten weather indicators data can be obtained.

**Table 1 Selected weather indicators**

Weather product	Max	90%	50%
$C$	✓	✓	✓
$E$	✓	✓	✓
$V$	✓	✓	✓
$\Delta Z$		✓	

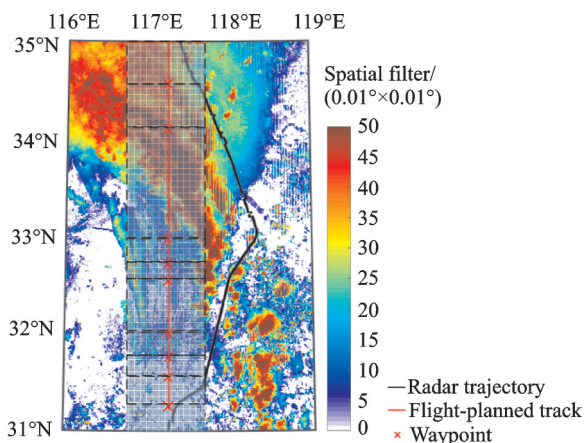


Fig.3 Spatial filter of trajectory segment

## 1.2 Radar trajectory data

The radar trajectory data with flight-related information are updated every 8 s. Every raw radar trajectory data file is used to record the trajectory point information of all flights in a certain airspace at every timestamp, including the call sign (flight ID), the ground speed, the height, the longitude, the latitude and other information. By processing the raw radar trajectory data, each flight trajectory can be obtained. Fig.4 shows some trajectories (red lines) on 17 August 2018 in China.



Fig.4 Radar trajectories on 17 August 2018 in China

To judge a whether flight deviated from the planned track, the historical trajectory point information is extracted from the raw radar trajectory data, including the timestamp, the flight ID, the latitude and the longitude, as shown in Table 2. For example, the second row in Table 2 represents that the timestamp of flight CBJ5131 was 22:04:45 on 17 August 2018, and its longitude was 113.136°, and its latitude was 22.922°.

**Table 2 Radar trajectory data sample**

Flight ID	Time stamp	Longitude/(°)	Latitude/(°)
CBJ5131	20180817220445	113.136	22.922
CBJ5131	20180817220453	113.130	22.910
CBJ5131	20180817220501	113.124	22.899

## 1.3 Flight plan data

The radar trajectory and the planned track of the same flight should be compared to judge whether flights avoided weather, which can cause a flight to deviate. The flight plan includes the flight ID, the departure time, the departure airport and the flight plan track, as shown in Table 3. The raw flight plan data are shown in Fig.5. The flight plan

**Table 3** Sample flight plan data

Flight ID	Departure airport	Departure time (date/time)	Flight plan track
CSZ9520	ZSSS	0628/0912	NXD A599 TOL H24 P25 H17 JDZ
CSH9280	ZSFY	0628/0908	FYG B208 HFE R343 SASAN
CQH8910	ZSQZ	0628/1022	ATSAB A470 LJG B221 SHZ G204 AND

flight ID	flight type	departure airport	departure time	arrival airport	arrival time	path
CSZ9520	S	ZSSS	0628/0912	ZSJD	0628/1012	NXD A599 TOL H24 P25 H17 JDZ
CSH9280	S	ZSFY	0628/0908	ZSSS	0628/1016	FYG B208 HFE R343 SASAN
CQH8910	S	ZSQZ	0628/0911	ZSSS	0628/1022	ATSAB A470 LJG B221 SHZ G204 AND
CXA8221	S	ZSQZ	0628/0907	ZSNJ	0628/1023	ATSAB A470 CJ/K0859S0980 W555 KAKIS W554 GOSRO
CDG8880	S	ZSOF	0628/0908	ZSYT	0628/1026	MADUK W73 NOBEM W95 OF W178 LAGAL H28 XDX W174 FD H101 P449
CBG7878	S	ZSRZ	0628/0955	ZSIN	0628/1033	P54 J166 WFG/M076S0750 H20 P291
CQA8822	S	ZSQD	0628/0912	ZSSS	0628/1035	XDX H28 LAGAL W178 OSIKI W166 ZJ W167 SASAN

Fig.5 Sample of raw flight plan data

track is composed of “waypoint-enroute-...-waypoint-enroute-waypoint” data.

## 2 Avoidance Predictor

The avoidance predictor of WAPM is to predict whether the flight needs to avoid weather based on forecast/actual weather by data mining. In this paper, each flight segment has ten weather indicators for the intensity of convective weather and the label represents whether the flight segment avoids weather. Thus the input of WAPM is ten weather

indicators, and the output is the avoidance weather classification label.

Fig.6 is the schematic of avoidance predictor. PCA<sup>[18]</sup> dimensional reduction first obtains the values of the ten weather indicators through weather data, and then each weather indicator is standardized to obtain the covariance matrix  $R$  and screen out the first  $p$  principal components. Avoidance label acquirement calculates the vertical distance between radar trajectory point with the 8 s update rate and flight plan track, and then the maximum

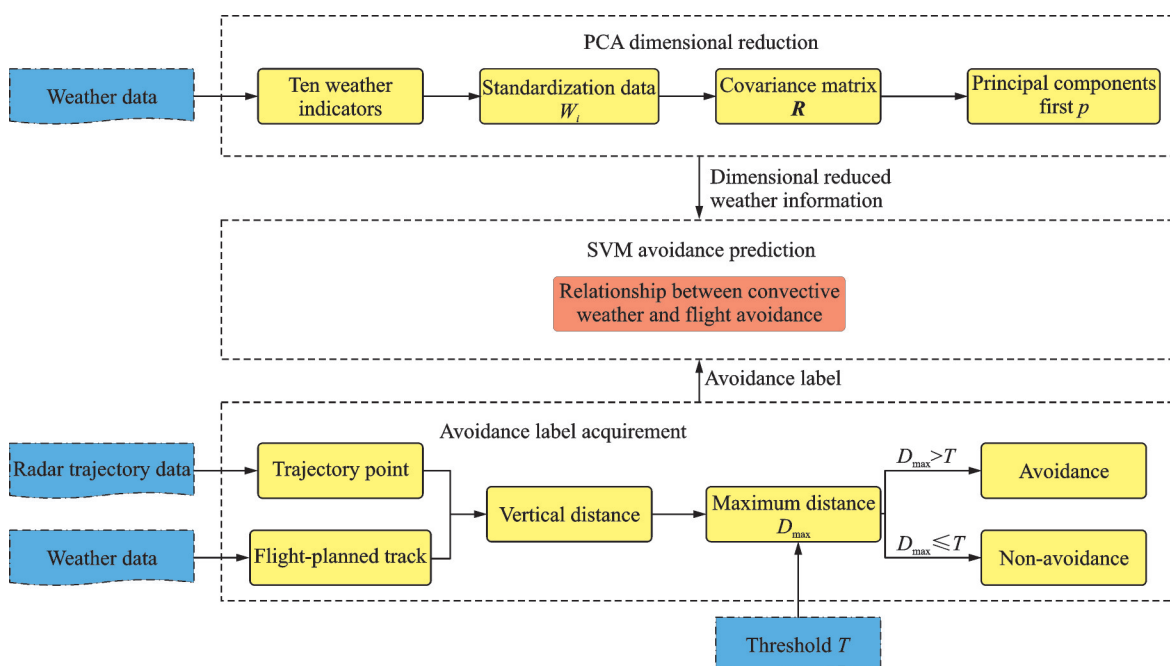


Fig.6 Schematic of avoidance predictor

distance of the vertical distance of each flight segment is obtained. By comparing with the selected threshold, the avoidance label of each flight segment can be obtained. Finally, the dimensional reduced weather information and avoidance label are input into the SVM algorithm to determine the relationship between convective weather and flight avoidance.

### 2.1 Avoidance label

Label setting is important for establishing a prediction model. In this paper, whether flight avoids weather is the label for model establishment. First, to label whether the flight avoids weather, the vertical distance between each radar trajectory point within each flight segment to the flight plan track is calculated. Second, the maximum calculated distance of each flight segment is compared with a threshold of 10 km to determine whether flights avoid weather. The threshold is 10 km because Article 15 of Chapter II of the basic rules of flight of the People's Republic of China<sup>[1]</sup> states that the width of enroute shall be 20 km and the width on each side of its centerline shall be 10 km. This avoidance result is preliminarily discriminated automatically. Then the preliminary result requires manual inspection through superimposed images of weather conditions, radar trajectory and flight plan track to validate the effectiveness of avoidance judgment process. If a flight avoids the weather, it will be labeled as "avoidance", otherwise it will be labeled as "non-avoidance". In Fig.7, two actual flight cases are shown. The red line is the flight plan track, the black line is the historical radar trajectory, and the colored area represents weather with different severities. Fig.7(a) shows that the flight diverts to avoid convective weather, and Fig. 7(b) shows that the flight does not divert. For each trajectory segment, the ten weather indicators can be acquired by percentiles selection in the spatial filter, as shown in Table 1. In this way, weather indicators and avoidance label data can be recorded.

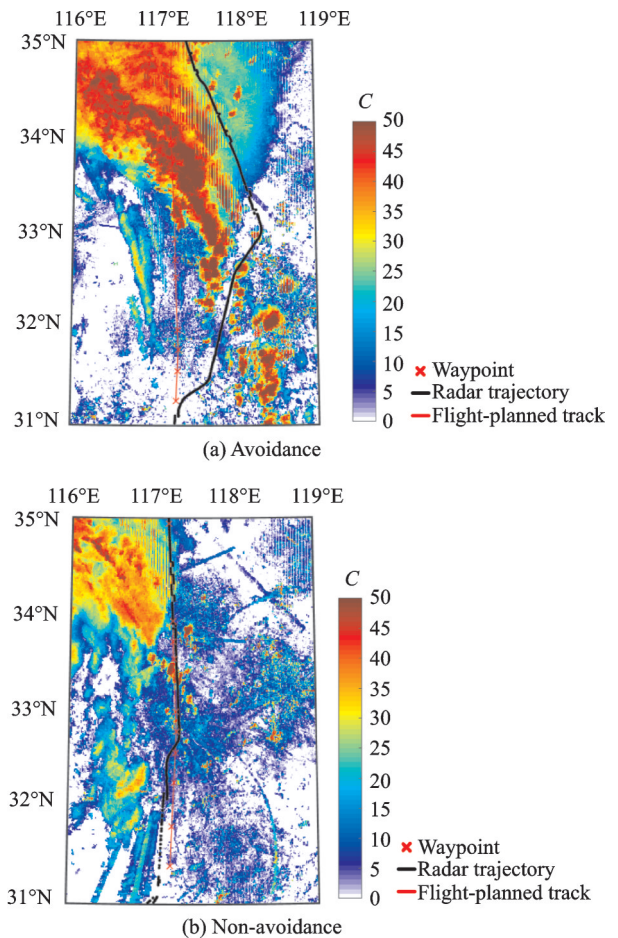


Fig.7 Flight segment classification

### 2.2 Dimension reduction

Based on results of data procession, there are ten weather indicators and avoidance label for every flight trajectory segment, described as

$$\begin{bmatrix} w_{11} & w_{12} & \cdots & w_{1m} & y_1 \\ w_{21} & w_{22} & \cdots & w_{2m} & y_2 \\ \vdots & \vdots & \ddots & \vdots & \vdots \\ w_{n1} & w_{n2} & \cdots & w_{nm} & y_n \end{bmatrix} = \begin{bmatrix} w_1 & w_2 & \cdots & w_m & y \end{bmatrix} \quad (2)$$

where  $w_{ij}$  is the weather indicator value, that is the value of weather indicator  $j$  of trajectory segment  $i$ ;  $w_j$  the vector of weather indicator  $j$ ;  $y_i$  the class label of trajectory segment  $i$ ;  $y$  the vector of class label;  $n$  the number of trajectory segment samples, and  $m$  the number of weather indicators. There are ten weather indicators, so  $m=10$ . Based on these data, WAPM will be established by data mining.

PCA is used for dimensionality reduction of weather indicators. First, standardization processing

is used for weather indicator data

$$W_{ij} = \frac{w_{ij} - \bar{w}_j}{S_j} \quad (3)$$

where  $w_{ij}$  is the value of weather indicator  $j$  of trajectory segment  $i$ ;  $\bar{w}_j$  the expectation of the weather indicator  $j$ ;  $S_j$  the standard deviation of the weather indicator  $j$ , and  $W_{ij}$  the value of standardized weather indicator  $j$  of trajectory segment  $i$ . The standardization weather indicator data can be represented by

$$\begin{bmatrix} W_{11} & W_{12} & \cdots & W_{1m} \\ W_{21} & W_{22} & \cdots & W_{2m} \\ \vdots & \vdots & \ddots & \vdots \\ W_{n1} & W_{n2} & \cdots & W_{nm} \end{bmatrix} = [W_1 \quad W_2 \quad \cdots \quad W_m] \quad (4)$$

Then, the covariance matrix of the weather indicators is obtained by Eqs.(5, 6), and the eigenvectors and eigenvalues can be acquired.

$$R = \begin{bmatrix} r_{11} & r_{12} & \cdots & r_{1m} \\ r_{21} & r_{22} & \cdots & r_{2m} \\ \vdots & \vdots & \ddots & \vdots \\ r_{m1} & r_{m2} & \cdots & r_{mm} \end{bmatrix} \quad (5)$$

where  $R$  is the covariance matrix formed by  $r_{ij}$ , which is the covariance between weather indicators  $i$  and  $j$ , calculated by Eq. (6), and  $m$  the number of weather indicators;  $n$  the number of trajectory segment samples.

$$r_{ij} = \frac{1}{n-1} \sum_{k=1}^n (W_{ki} - \bar{W}_i)(W_{kj} - \bar{W}_j) \quad (6)$$

Next,  $m$  eigenvalues  $\lambda$  of the covariance matrix  $R$  can be calculated, and sorted from the largest to the smallest. The corresponding eigenvectors are represented as  $a$ , described in Eq. (7). To retain most information from the original weather indicator data, the first  $p$  eigenvectors of eigenvalues whose cumulative contribution rate ( $C_c$ ) greater than 90% are extracted to form the transformation matrix  $T$ , as shown in Eq. (10). The  $C_c$  is calculated according to Eq.(8), where  $\lambda_k$  is the  $k$ th eigenvalue, and the first  $p$  principal components can be calculated by Eq. (9), where  $W_j$  is the value of standardized weather indicator  $j$ . Thus the dimensionally reduced data, which reflects 90% of the information, can be obtained by the transformation matrix  $T$ .

$$a_1 = \begin{bmatrix} a_{11} \\ a_{21} \\ \vdots \\ a_{m1} \end{bmatrix}, a_2 = \begin{bmatrix} a_{12} \\ a_{22} \\ \vdots \\ a_{m2} \end{bmatrix}, \cdots, a_m = \begin{bmatrix} a_{1m} \\ a_{2m} \\ \vdots \\ a_{mm} \end{bmatrix} \quad (7)$$

$$C_c = \frac{\sum_{k=1}^i \lambda_k}{\sum_{k=1}^m \lambda_k} \quad i = 1, 2, \cdots, m \quad (8)$$

$$F_i = a_{1i}W_1 + a_{2i}W_2 + \cdots + a_{mi}W_m \quad (9)$$

$$i = 1, 2, \cdots, p$$

$$T = \begin{bmatrix} a_{p1} \\ a_{p2} \\ \vdots \\ a_p \end{bmatrix} \quad (10)$$

### 2.3 Avoidance prediction

In this paper, the weather indicator data are used as classification factors, and the avoidance information is used as the classification label results. SVM<sup>[19]</sup> is used for classification. As shown in Fig.8, we assumed that the green circles represent the non-avoidance segments, the orange triangles represent the avoidance segments, and the axes represent the weather indicator values. To classify avoidance and non-avoidance segments, the hyperplane can maximize the distance between the nearest data points of the two classification samples, which needs to be determined by SVM supervised learning. In Fig. 8, the blue dotted line shows the position of the nearest data points of the two classifications, and the purple line represents the hyperplane.

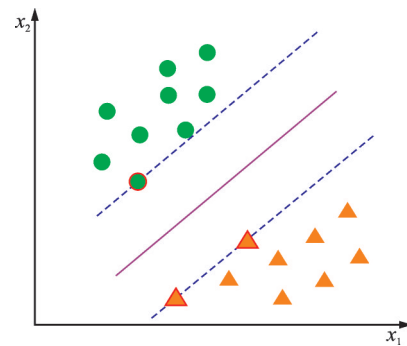


Fig.8 Machine learning classification model

The optimization objective function of SVM can be expressed as

$$\begin{cases} \max W(a) = \sum_{i=1}^n a_i - \frac{1}{2} \sum_{i,j=1}^n a_i a_j y_i y_j K(x_i, x_j) \\ 0 \leq a_i \leq c \\ \sum_{j=1}^n a_j y_j = 0 \end{cases} \quad (11)$$

where  $a$  is the introduced Lagrangian multiplier;  $a_i$  and  $a_j$  are the  $i$ th and  $j$ th Lagrangian multipliers;  $(x_i, y_i)$  is data of trajectory segment  $i$ ,  $x_i$  is the weather indicator data, and  $y_i$  is the avoidance label data,  $x_i$  and  $x_j$  are the  $i$ th and  $j$ th support vectors, and  $y_i$  and  $y_j$  are class labels for  $x_i$  and  $x_j$ . The value of  $y_i$  and  $y_j$  is in  $\{-1, 1\}$ . In this paper,  $-1$  indicates non-avoidance, and  $1$  indicates avoidance.  $c$  is the penalty factor, which is a hyperparameter. The RBF kernel function is selected as  $K(x_i, x_j)$ , as shown in Eq. (12). The essence of RBF is to map every sample point to an infinite dimensional eigenspace, which makes linearly inseparable data linearly separable.

$$K(x_i, x_j) = \exp(-\gamma \|x_i - x_j\|^2) \quad (12)$$

where  $\gamma$  is the RBF width hyperparameter, and  $\|x_i - x_j\|$  the modulus of difference between support vector  $x_i$  and  $x_j$ .

To get flight segment classification, the weather data  $x$  can be used in Eq. (13) to obtain the classification result of the flight segment.

$$f(x) = \text{sgn}\left(\sum_{i=1}^n y_i a_i K(x \cdot x_i) + b^*\right) \quad (13)$$

$$\text{sgn}(h) = \begin{cases} +1 & h \geq 0 \\ -1 & h < 0 \end{cases} \quad (14)$$

where  $b^*$  is the displacement term that determines the distance between the hyperplane and the origin, and  $\text{sgn}$  a sign function.

### 3 Evaluation

Evaluation of WAPM is divided as verification and analysis. To avoid model overfitting, verification is to determine the appropriate parameters in the model establishment. And the prediction ability of WAPM is analyzed by comparing it with other methods.

#### 3.1 Verification

In this paper, 6 146 flights, including 18 870 flight trajectory segments from 9:00 to 16:00 on 11 to 20 August 2018 in the eastern and the central southern China are selected as the training and the testing datasets for modeling, as shown in Table 4.

**Table 4 Recorded flight segment number**

Date	Flight number	Flight segment number	Avoidance number	Non-avoidance number
0811	511	1 525	887	638
0812	520	1 534	994	540
0813	591	2 131	1 230	901
0814	545	1 654	855	799
0815	785	2 982	1 699	1 283
0816	850	3 260	1 850	1 410
0817	600	1 870	656	1 214
0818	717	1 733	1 065	668
0819	532	1 208	672	536
0820	495	973	595	378
Total	6 146	18 870	10 503	8 367

By comparing the flight plan tracks with radar trajectories, avoidance label of “ $-1$ ” and “ $1$ ”, and weather indicator data  $E_{\max}$ ,  $50\%E$ ,  $90\%E$ ,  $V_{\max}$ ,  $50\%V$ ,  $90\%V$ ,  $C_{\max}$ ,  $50\%C$ ,  $90\%C$  and  $\Delta Z$  for 18 870 flight trajectory segments were recorded, as shown in Table 5, which shows five samples. In Table 5, the first ten columns are the values of ten weather indicators, which represent the weather condition, and the last column is the avoidance label: “ $1$ ” indicates avoidance, and “ $-1$ ” indicates non-avoidance.

According to Eq. (3), the weather indicator data from 18 870 flight trajectory segments were processed and standardized. The data in Table 6 are the results of the standardization of the weather indicator data in Table 5.

**Table 5 Recorded flight segment data**

Segment	$E_{\max}$	$50\%E$	$90\%E$	$V_{\max}$	$50\%V$	$90\%V$	$C_{\max}$	$50\%C$	$90\%C$	$\Delta Z$	Label
1	6.04	1.16	2.74	8.43	7.02	7.37	46.50	32.00	38.50	5 740.00	1
2	9.16	1.23	3.57	8.68	6.81	8.25	48.00	34.00	42.00	-1 856.57	1
3	3.52	0.84	2.20	14.58	6.75	7.30	42.00	30.50	37.50	2 482.00	-1
4	10.96	0.41	4.12	9.09	4.77	6.01	50.00	27.00	45.00	3 164.00	1
5	3.07	0.19	0.48	11.46	8.51	9.42	50.00	21.50	25.00	-2 281.91	-1

**Table 6 Weather indicator data after standardization**

$E_{\max}$	50% $E$	90% $E$	$V_{\max}$	50% $V$	90% $V$	$C_{\max}$	50% $C$	90% $C$	$\Delta Z$
-0.48	-0.12	-0.45	-0.18	0.60	0.02	0.26	0.55	0.24	0.82
-0.25	-0.09	-0.32	-0.14	0.55	0.20	0.34	0.68	0.44	-0.52
-0.67	-0.38	-0.54	0.83	0.54	0.00	0.02	0.45	0.18	0.25
-0.12	-0.48	-0.22	-0.07	0.06	-0.27	0.44	0.21	0.61	0.37
-0.70	-0.59	-0.82	0.32	0.96	0.45	0.44	-0.16	-0.53	-0.60

To begin, 70% of the total sample data were used for modeling as the training dataset, and the other 30% of total sample data were used for testing the established model as the testing dataset. The dataset was divided randomly. The eigenvalue and contribution rate of each weather indicator

using the training dataset was obtained by Eqs. (5, 6, 8). The results of descending order are shown in Table 7. The  $C_c$  of the first four components was up to 92.57%, which demonstrates that the first four components has obtained 90% of the information.

**Table 7 Eigenvalue and contribution rate of component**

Serial number	Eigenvalue	Contribution rate/%	$C_c$ /%
1	7.22	72.17	72.17
2	0.93	9.33	81.50
3	0.74	7.40	88.90
4	0.37	3.67	92.57
5	0.26	2.62	95.19
6	0.23	2.30	97.49
7	0.10	0.97	98.46
8	0.07	0.71	99.17
9	0.07	0.65	99.82
10	0.02	0.18	100.00

To validate the effectiveness of PCA and the number of eigenvalues, modeling time and accuracy on testing dataset of six feature selections were calculated, as shown in Table 8. As can be seen, using ten weather indicators after PCA costed less modeling time than using ten weather indicators without PCA. The modeling time and accuracy on

the testing dataset both increased as the number of principal components increased. To obtain the trade-off between modeling time and accuracy on the testing dataset, the first four principal components were selected for subsequent analysis.

The eigenvectors of the first four components were extracted to form the transformation matrix

**Table 8 Modeling time and accuracy on testing dataset of different feature selections**

Serial number	Feature selection	Modeling time/s	Accuracy on testing dataset/%
1	10 weather indicators without PCA	10.56	85.89
2	10 weather indicators after PCA	8.91	85.89
3	Weather indicators calculated by the first 3 principal components	6.97	81.6
4	Weather indicators calculated by the first 4 principal components	7.43	84.94
5	Weather indicators calculated by the first 5 principal components	7.74	85.19
6	Weather indicators calculated by the first 6 principal components	7.97	85.41

in Eq.(15). As can be seen, the values of the first nine columns of the first component are above 0. The first nine columns represent different quantile values of  $E$ ,  $V$  and  $C$ , which indicates the severe degree of convective weather. Thus the first component can be named as “Severe degree of convective weather component”. The second component had strong positive correlations with the seventh, the eighth and the ninth columns. These three columns represent different quantile values of  $C$ , thus the second component can be named as

$$\begin{bmatrix} 0.321 & 0.340 & 0.347 & 0.323 & 0.306 & 0.352 & 0.284 & 0.262 & 0.309 & -0.307 \\ -0.391 & 0.024 & -0.265 & -0.255 & 0.190 & -0.161 & 0.199 & 0.634 & 0.411 & 0.194 \\ 0.113 & -0.338 & 0.037 & 0.030 & -0.485 & -0.054 & 0.664 & -0.227 & 0.370 & 0.066 \\ 0.402 & 0.289 & 0.307 & -0.053 & -0.099 & -0.173 & -0.034 & 0.128 & -0.037 & 0.774 \end{bmatrix} \quad (15)$$

Then, the dimensional reduction weather indicator data transformed through the transformation matrix were used for modeling classification by SVM. The training process was to determine appropriate penalty factor  $c$  and the radial basis parameters  $\gamma$ . To avoid overfitting while using 70% of total sample data (training dataset), we adopted ten-fold cross validation<sup>[20]</sup>. The training dataset was randomly divided into ten parts, nine of which were used as the training sets, and the remaining one part was used as the validation set. After ten experimental tests, the average accuracy of was used as the final evaluation index. With different values of  $c$  and  $\gamma$ , the accuracy of the data classification was calculated. Finally, the parameter pair of  $c$  and  $\gamma$  with the highest accuracy was selected. By using “grid search CV” in Python, the final parameter pairs selected by this model were  $c=2.575$  and  $\gamma=0.5$ . The classification accuracy of this parameter pair was 84.95%.

### 3.2 Analysis

To describe the predictive ability of WAPM, four prediction evaluation indexes, including the prediction accuracy ( $A$ ), precision ( $P$ ) and recall ( $R$ ) and  $F_1$ <sup>[21]</sup>, were selected.  $A$  is the ratio of the number of correctly predicted samples to the total number of samples, as shown in Eq.(16).  $P$  and  $R$  are obtained by the statistical confusion matrix. According to the combination of its real category and learn prediction category, the samples can be divided

“ $C$  component”. The third component has strong negative correlations with the second the fifth and the eighth columns. These three columns represent the 50% values of  $E$ ,  $V$  and  $C$ , thus the third component can be named as “50% value component”. The fourth component has strong positive correlations with the first, the second, the third and the tenth columns. These four columns represent different quantile values of  $E$  and  $\Delta Z$ , thus the fourth component can be named as “ $E$  and  $\Delta Z$  component”.

into four cases in the binary classification problem: True positive (TP), false positive (FP), true negative (TN) and false negative (FN).  $P$  is the proportion of true avoidances in the samples that are predicted to be diverted, as shown in Eq.(17).  $R$  is the proportion of true avoidances in the samples that are actually diverted, as shown in Eq.(18). When  $P$  is high,  $R$  tends to be low, and when  $R$  is high,  $P$  is low; thus, these measures are contradictory, but  $F_1$  can balance the relationship of the two, as shown in Eq.(19).

$$A=(TP+TN)/(TP+FN+FP+TN) \quad (16)$$

$$P=TP/(TP+FP) \quad (17)$$

$$R=TP/(TP+FN) \quad (18)$$

$$F_1=2 \times P \times R / (P+R) \quad (19)$$

Delaura et al. used GDA and kNN methods to establish weather avoidance prediction models in 2006<sup>[3]</sup> and 2008<sup>[4]</sup>, which had a similar function with WAPM for avoidance prediction. In addition, the logistic regression (LR), the random forest (RF) and the deep neural network (DNN) methods are also common machine learning algorithms, which are used to learn and summarize from the known data. Therefore, these four methods are compared with WAPM in terms of the four evaluation indexes:  $A$ ,  $P$ ,  $R$  and  $F_1$ .

#### 3.2.1 GDA

The prediction model was established using GDA by Delaura, et al.<sup>[3]</sup>. The prerequisite for using GDA is that the segment sample data needs to

be subject to Gaussian distribution. Unfortunately, from the paper published by Delaura et al.<sup>[3]</sup>, they used 490 planned trajectories to establish the model, but there was no Gaussian verification processing. When using GDA in this paper, the Jacques-Bella test (JBTest) was used to test the Gaussian distribution of each sample weather indicator data with a 90% confidence level. For the same comparison, this paper used samples from 11 to 20 August

2018, and the whole samples from the ten days were used to test the Gaussian distribution. The JBTest function in MATLAB was used to verify whether the data of each weather indicator obey the Gaussian distribution. Fig.9 shows the Gaussian distribution test for the samples from 17 August, and Table 9 shows the results of the samples from 17 August. So GDA is not applicable to weather avoidance prediction in China.

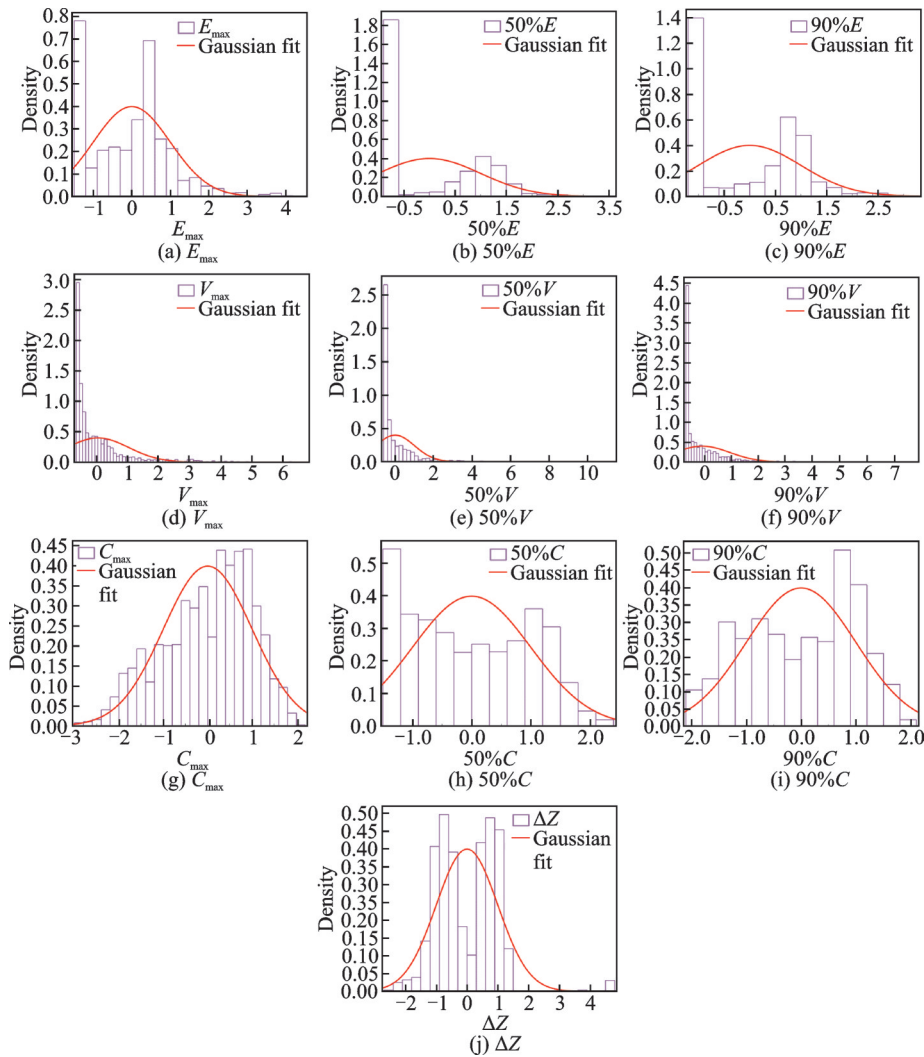


Fig.9 Gaussian distribution test samples from 17 August 2018

**Table 9 Gaussian distribution test results for samples from August 17 2018**

Weather indicator	$E_{max}$	50%E	90%E	$V_{max}$	50%V
Obey Gaussian distribution or not	N	N	N	N	N
Weather indicator	90%V	maxC	50%C	90%C	$\Delta Z$
Obey Gaussian distribution or not	no	no	no	no	no

The test results reflected that GDA does not apply to the Chinese flight trajectories, and Delaura

et al. failed to verify the Gaussian distributions and misused GDA.

### 3.2.2 kNN, LR, RF and DNN

Delaura et al.<sup>[3-4]</sup> also used the kNN method to establish weather avoidance prediction model, and the number of neighbors  $k$  was determined to be four. So  $k = 4$  was used to establish the WAPM. The distance metric of kNN is Euclidean distance. For LR, the classification learner tool from MATLAB was used to establish the logistic regression model. For RF, among the commonly used decision tree algorithms ID3, C4.5 and CART, CART with the highest accuracy on the test dataset was selected and the split criterion was the Gini index. For DNN, the neural pattern recognition tool from MATLAB was used to establish the DNN model. After several experiments and parameter tuning,

the parameters when the highest accuracy on the test dataset was reached were obtained. The number of hidden layers was 10 and the number of hidden neurons in each hidden layer was 10. The training algorithm was the scaled conjugate gradient backpropagation algorithm. The performance function was crossentropy. The learning rate was 0.01. The maximum epoch was 1 000 and the validation checks was 6. While using above four algorithms, ten-fold cross validation was adopted on 70% of the total sample data (training dataset) to avoid overfitting. The confusion matrix is shown in Table 10. The confusion matrix was obtained by using 30% of the total sample data as the test dataset by the established model of kNN, LR, RF, DNN and WAPM.

**Table 10 Confusion matrix for kNN, LR, RF, DNN and WAPM**

True condition	Prediction condition									
	kNN		LR		RF		DNN		WAPM	
	Avoidance	Non-avoidance	Avoidance	Non-avoidance	Avoidance	Non-avoidance	Avoidance	Non-avoidance	Avoidance	Non-avoidance
Avoidance	2 052(TP)	693(FN)	2 155(TP)	590(FN)	2 162(TP)	583(FN)	2 201(TP)	544(FN)	2 163(TP)	582(FN)
Non-avoidance	408(FP)	2 277(TN)	370(FP)	2 315(TN)	357(FP)	2 328(TN)	329(FP)	2 356(TN)	235(FP)	2 450(TN)

$P$ ,  $R$  and  $F_1$  values for kNN, LR, RF, DNN and WAPM were calculated by Eqs.(17—19), and

values of  $A$ ,  $P$ ,  $R$  and  $F_1$  for these five methods were obtained, as shown in Table 11.

**Table 11 Evaluation indicators of kNN, LR, RF, DNN and WAPM**

Evaluation index	kNN	LR	RF	DNN	WAPM
$A/\%$	79.73	82.32	82.69	83.92	84.95
$P/\%$	83.41	85.01	85.83	86.99	90.20
$R/\%$	74.75	77.75	78.76	80.18	78.80
$F_1/\%$	78.84	82.43	82.14	83.44	84.12

To reflect a clear difference between the four indexes of the five methods, Fig.10 presents the data from Table 11 in a histogram.

For kNN and WAPM, Delaura et al.<sup>[4]</sup> did not directly give kNN prediction accuracy in his published paper. The paper only pointed out that the accuracy of GDA was 75% and concluded that the prediction accuracy of kNN was less than that of GDA. Table 11 shows that kNN's accuracy is indeed relatively low with only 79.73%, while this value for

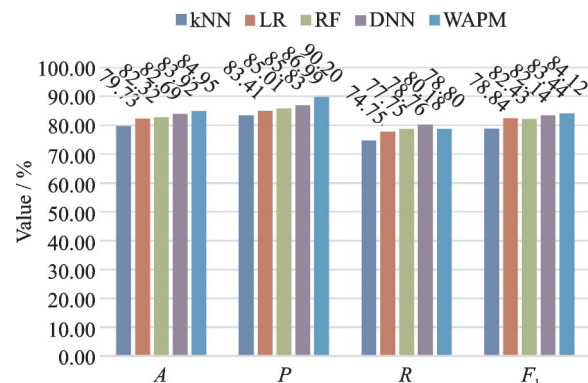


Fig.10 Index histogram chart

WAPM can reach 84.95%, 5.22% greater than that of kNN. The  $P$  value of WAPM is 90.20%, 6.79% more than that of kNN, which indicates that WAPM has a higher proportion of actual weather avoidance. The  $R$  value of WAPM is 78.80%, 4.05% greater than that of kNN, indicating that WAPM has a higher proportion of accurate weather avoidance prediction. Further, the  $F_1$  value of WAPM is 84.12%, 5.28% greater than that of kNN, which indicates that the prediction ability of WAPM is better.

Similarly, the  $A$ ,  $P$ ,  $R$  and  $F_1$  values of WAPM are all slightly better than those of the other three methods, so the prediction ability of WAPM is better than the other three methods. Based on the four valuation indexes, WAPM has a greater predictive ability in China's operating environment.

## 4 Conclusions

Based on weather products, ten weather indicators are used to reflect convective weather. Data mining along with weather data, radar trajectory data and flight plan data from 18 870 flight trajectory segments of 6 146 flights from 9:00 to 16:00 on 11 to 20 August, 2018 in the eastern and the central southern China are used to establish WAPM. The results of WAPM are compared with those of GDA, kNN, LR, RF and DNN, and the following conclusions can be drawn.

(1) The data of each weather indicator do not obey Gaussian distribution, so the GDA proposed in Refs.[3-4] cannot be used and does not apply to the weather avoidance prediction of convective weather in China.

(2) WAPM's accuracy is 84.95%, and those of kNN, LR, RF and DNN are 79.73%, 82.32%, 82.69% and 83.92%, respectively. WAPM is more accurate.

(3) WAPM has a greater  $F_1$  value, which indicates that its predictive ability is more accurate than those of kNN, LR, RF and DNN.

(4) The WAPM and DNN are similar, but the predictive ability of WAPM is slightly better than that of DNN.

The WAPM's prediction result is better than those of kNN, LR, RF and DNN but not too accurate. There are two possible reasons for this.

One is that other weather products (such as wind speed, lightning and other parameters) can be taken into account in further work. By using different weather products, the state of convective weather can be reflected from different aspects. With more weather indicators, the dimensionality reduction process will be more complex, so a new improved dimensionality reduction method need to be studied.

Further, the recorded radar trajectory data were partially missed, and manual inspection is required when processing the trajectory, so additional methods for automatically inspecting trajectories should be studied in future work.

In addition, additional research into path re-routing should also be undertaken to provide pilots and controllers with direct decision-making basis to improve airspace utilization and flight safety. In this paper, the actual historical weather data corresponding to the flight trajectory are used, but actual operations forecast weather data are not used. This discrepancy may cause uncertainty in weather avoidance prediction, so it is necessary to correlate forecast weather data with WAPM in future work.

## References

- [1] Civil Aviation Administration of China. Development statistics Bulletin of Civil Aviation Industry in 2019[R]. Beijing: Civil Aviation Administration of China, 2020.
- [2] MCNALLY D, SHETH K, GONG C, et al. Operational evaluation of dynamic weather routes at American airlines[C]//Proceedings of the 10th USA / Europe Air Traffic Management research and Development Seminar (ATM2013). Chicago, America: FAA, 2013.
- [3] DELAURA R, EVANS J. Exploratory study of modeling enroute pilot convective storm flight deviation behavior[C]//Proceedings of the 12th Conference on Aviation Range and Aerospace Meteorology. Atlanta, America: AMS, 2006.
- [4] DELAURA R, ROBINSON M, PAWLAK M, et al. Modeling convective weather avoidance in enroute airspace[C]//Proceedings of the 13th Conference on

- Aviation, Range, and Aerospace Meteorology. New Orleans, America: AMS, 2008.
- [5] STEWART T, DEARMON J, CHALOUX D. Using flight information to improve weather avoidance predictions[C]//Proceedings of 2013 Aviation Technology, Integration & Operations Conference. Los Angeles, America: AIAA, 2013: 2013-4377.
- [6] MATTHEWS M, DELAURA R. Evaluation of enroute convective weather avoidance models based on planned and observed flights[C]//Proceedings of the 14th Conference on Aviation, Range, and Aerospace Meteorology. Atlanta, America: AMS, 2010.
- [7] CAMPBELL S, MATTHEWS M, DELAURA R. Evaluation of the convective weather avoidance model for arrival traffic[C]//Proceedings of the 12th AIAA Aviation Technology, Integration, and Operations (ATIO) Conference and the 14th AIAA/ISSMO. Indianapolis, America: AIAA, 2012: 2012-5500.
- [8] MATTHEWS M, VEILLETTE M, VENUTI J, et al. Heterogeneous convective weather forecast translation into airspace permeability with prediction intervals[J]. Journal of Air Transportation, 2016, 24(2): 41-54.
- [9] YE Z, GAO W, WANG L, et al. Airspace blocking probability model and traffic obstruction index model under convective weather[J]. Aeronautical Computing Technique, 2014, 44(2): 1-6.
- [10] ZHU G. Centralized disaggregate stochastic allocation models for collaborative trajectory options program (CTOP)[C]//Proceedings of 2018 IEEE/AIAA 37th Digital Avionics Systems Conference (DASC). London, UK: IEEE, 2018: 1-10.
- [11] HENTZEN D, KAMGARPOUR M, SOLER M, et al. On maximizing safety in stochastic aircraft trajectory planning with uncertain thunderstorm development[J]. Aerospace Science and Technology, 2018, 79: 543-553.
- [12] KICINGER R, KROZEL J, STEINER M, et al. Airport capacity prediction integrating ensemble weather forecasts[C]//Proceedings of AIAA Infotech@Aerospace 2012 Conference. Garden Grove, USA: AIAA, 2012: 2012-2493.
- [13] ARNESON H, BOMBELLI A, SEGARRA-TORNÉ A, et al. Analysis of convective weather impact on pre-departure routing of flights from fort worth center to new york center[C]//Proceedings of the 17th AIAA Aviation Technology, Integration, and Operations Conference. Denver, USA: AIAA, 2017: 2017-3593.
- [14] ZHU G. En route flight time prediction under convective weather events[C]//Proceedings of 2018 Aviation Technology, Integration & Operations Conference. Atlanta, USA: AIAA, 2018: 2018-3670.
- [15] CHEN Z, LIN Y, YANG B. Study on algorithm for rerouting based on historical data[J]. Advanced Engineering Sciences, 2018, 50(4): 110-115.
- [16] DU S, WANG J, REN J. On the aircraft flying-goal diversion based on the improved multi-objective particle swarm optimization[J]. Journal of Safety and Environment, 2020, 20(1): 177-158.
- [17] FU H. Application of meteorological radar products in observation and forecast of strong convection weather[J]. South China Agriculture, 2018, 12(21): 148-149.
- [18] ZHAO Q. A review of component analysis[J]. Software Engineer, 2016, 19(6): 1-3.
- [19] LIANG L, ZHONG Z, CHEN Z. Research and simulation of kernel function selection for support vector machine[J]. Computer Engineering & Science, 2015, 37(6): 1135-1141.
- [20] YANG L, WANG Y. Survey for various cross-validation estimators of generalization error[J]. Application Research of Computers, 2015, 32(5): 1287-1297.
- [21] YUAN F, LIN J, DENG Y, et al. Solar flare forecasting model of combining principal component analysis with support vector machine[J]. Chinese Science Bulletin, 2016, 61(20): 2316-2321.
- Acknowledgement** This work was supported by Nanjing University of Aeronautics and Astronautics Graduate Innovation Base (Laboratory) Open Fund (No. kfjj20200710).
- Authors** Mr. LI Jiahao received B.E. degree from Civil Aviation of China, Tianjin. From 2019, he is a postgraduate student in Nanjing University of Aeronautics and Astronautics, researching in transportation engineering.
- Dr. WANG Shijin received the Ph.D. degree in transportation engineering from Nanjing University of Aeronautics and Astronautics in 2011, and finished her postdoctoral career in 2017. Her research includes air traffic planning and management, and air traffic safety analysis.
- Author contributions** Mr. LI Jiahao designed the study and established the model. Dr. WANG Shijin contributed to the introduction and background of the study. Ms. CHU Jiewen contributed to the data preparation of the study. Ms. LIN Jingjing used several algorithms for validation and analysis. Mr. WEI Chunjie contributed to the conclusions

and future work of the study. All authors commented on the manuscript draft and approved the submission.

**Competing interests** The authors declare no competing interests.

(Production Editor: ZHANG Bei)

## 基于支持向量机的航路空域内对流天气避让预测

李家豪<sup>1</sup>, 王世锦<sup>1</sup>, 储洁雯<sup>1</sup>, 林荆荆<sup>2</sup>, 魏纯洁<sup>3</sup>

(1. 南京航空航天大学民航学院, 南京 211106, 中国; 2. 南京莱斯信息技术股份有限公司, 南京 210014, 中国;

3. 中国民用航空华东地区空中交通管理局江苏分局, 南京 211113, 中国)

**摘要:** 随着全球空中交通的快速发展, 航班延误问题越来越严重。对流天气是造成航班延误的主要原因之一, 已经影响到民航行业的可持续发展, 成为一个社会问题。如果能够提前预测与天气有关的航班是否改航, 那么空中交通活动的参与者就可以协调调度, 极大减少航班延误。本文提出了天气避让预测模型 (Weather avoidance prediction model, WAPM), 以寻找天气与飞行轨迹之间的关系, 并基于历史飞行数据预测未来航班是否改航。由于天气数据量大, 采用主成分分析对 10 维天气指标进行降维以提取 90% 的信息。然后通过确定径向基函数的超参数  $c$  和  $\gamma$ , 利用支持向量机来预测飞行是否改航。最后, 通过预测准确率、精度、查全率和  $F_1$  评价模型性能, 并与  $k$  近邻 ( $k$  nearest neighbor, kNN)、逻辑回归 (Logistic regression, LR)、随机森林 (Random forest, RF) 和深度神经网络 (Deep neural network, DNN) 进行比较。对于准确率, WAPM 比 kNN、LR、RF 和 DNN 方法分别高 5.22%、2.63%、2.26% 和 1.03%; 对于精度, WAPM 比 kNN、LR、RF 和 DNN 方法分别大 6.79%、5.19%、4.37% 和 3.21%; 对于查全率, WAPM 比 kNN、LR、RF 分别大 4.05%、1.05%、0.04%, 比 DNN 低 1.38%; 对于  $F_1$ , WAPM 比 kNN、LR、RF 和 DNN 方法分别高 5.28%、1.69%、1.98% 和 0.68%。

**关键词:** 对流天气; 避让预测; 数据挖掘; 评价指标; 航路空域